

Fast noncontact measurements of tablet dye concentration

Ervin Nippolainen,¹ Tuomas Ervasti,² Laure Fauch,¹ Serguei V. Miridonov,³ Jarkko Ketolainen,² and Alexei A. Kamshilin¹

¹Department of Physics and Mathematics, University of Eastern Finland, P.O.Box 1627, FIN-70211 Kuopio, Finland

²Department of Pharmacy, University of Eastern Finland, P.O.Box 1627, FIN-70211 Kuopio, Finland

³Optics Department, Centro de Investigación Científica y de Educación Superior de Ensenada, C.P. 22860, A.P. 360, Ensenada, B.C.Mexico

Ervin.Nippolainen@uef.fi

Abstract: A non-contact, non-destructive technique for estimating the dye concentration of a tablet is presented. These measurements are performed by an optoelectronic system capable for fast acquisition of two-dimensional distribution of reflection spectra with high spatial resolution by using a subspace vector model of surface reflection. Vector components representing compressed spectral data are used directly (without reconstruction of the reflection spectra) for discrimination of tablets with small dye-concentration difference. Analysis of the data obtained after tablet illumination by 7 mutually orthogonal spectral functions allows us to find a single optimal spectral function which is enough for estimating the dye concentration. Using the optimal spectral function, either the mean concentration of riboflavin or distribution of the concentration over the tablet surface can be evaluated with high rate which ensures application of the technique for online quality control of each tablet.

©2010 Optical Society of America

OCIS codes: (330.0330) Vision, color, and visual optics; (330.6180) Spectral discrimination; (110.4234) Multispectral and hyperspectral imaging; (100.5010) Pattern recognition.

References and links

1. J. Barra, A. Ullrich, F. Falson-Rieg, and E. Doelker, "Color as an indicator of the organization and compactibility of binary powder mixes," *Pharm. Dev. Technol.* **5**(1), 87–94 (2000).
2. S. Vemuri, C. Taracatac, and R. Skluzacek, "Color stability of ascorbic acid tablets measured by tristimulus colorimeter," *Drug Dev. Ind. Pharm.* **11**(1), 207–222 (1985).
3. G. Stark, J. P. Fawcett, I. G. Tucker, and I. L. Weatherall, "Instrumental evaluation of color of solid dosage forms during stability testing," *Int. J. Pharm.* **143**(1), 93–100 (1996).
4. J. Berberich, K.-H. Dee, Y. Hayauchi, and C. Pörtner, "A new method to determine discoloration kinetics of uncoated white tablets occurring during stability testing—an application of instrumental color measurement in the development pharmaceuticals," *Int. J. Pharm.* **234**(1-2), 55–66 (2002).
5. P. D. Oram, and J. Strine, "Color measurement of a solid active pharmaceutical ingredient as an aid to identifying key process parameters," *J. Pharm. Biomed. Anal.* **40**(4), 1021–1024 (2006).
6. J. Subert, and J. Cizmárik, "Application of instrumental colour measurement in development and quality control of drugs and pharmaceutical excipients," *Pharmazie* **63**(5), 331–336 (2008).
7. M. Bornstein, "Color and its measurements," *J. Soc. Cosmet. Chem.* **19**, 649–667 (1968).
8. A. A. Kamshilin, and E. Nippolainen, "Chromatic discrimination by use of computer controlled set of light-emitting diodes," *Opt. Express* **15**(23), 15093–15100 (2007).
9. L. T. Maloney, and B. A. Wandell, "Color constancy: a method for recovering surface spectral reflectance," *J. Opt. Soc. Am. A* **3**(1), 29–33 (1986).
10. J. Cohen, "Dependency of the spectral reflectance curves of the Munsell color chips," *Psychon. Sci.* **1**, 369–370 (1964).
11. *Munsell book of color, matte edition*, (Munsell Color, Baltimore, Md., 1976).
12. J. P. S. Parkkinen, J. Hallikainen, and T. Jaaskelainen, "Characteristic spectra of Munsell colors," *J. Opt. Soc. Am. A* **6**(2), 318–322 (1989).
13. T. Jaaskelainen, J. P. S. Parkkinen, and S. Toyooka, "Vector-subspace model for color representation," *J. Opt. Soc. Am. A* **7**(4), 725–730 (1990).
14. D. H. Marimont, and B. A. Wandell, "Linear models of surface and illuminant spectra," *J. Opt. Soc. Am. A* **9**(11), 1905–1913 (1992).

15. H. Du, R. A. Fuh, J. Li, A. Corkan, and J. S. Lindsey, "PhotochemCAD: A computer-aided design and research tool in photochemistry," *Photochem. Photobiol.* **68**, 141–142 (1998).
 16. L. Fauch, E. Nippolainen, A. A. Kamshilin, M. Hauta-Kasari, J. P. S. Parkkinen, and T. Jaaskelainen, "Optical implementation of precise color classification using computer controlled set of light emitting diodes," *Opt. Rev.* **14**(4), 243–245 (2007).
 17. L. Fauch, V. Y. Teplov, E. Nippolainen, and A. A. Kamshilin, "Fast acquisition of reflectance spectra using wide spectral lines," *Opt. Rev.* **16**(4), 472–475 (2009).
-

1. Introduction

Variation of ingredients concentration of tablets leads to a change of their reflection spectra, which is visually recognized as a change of color [1]. Therefore, measurements of surface color are frequently used in development, stability testing, production, and quality control of synthetic and natural drugs [2–6]. Quantitatively the change of the surface color is monitored and measured by using conventional tristimulus colorimetry techniques [7]. However in many practical cases, color changes are smaller than the sensitivity of colorimetric methods. Moreover, very often variations of the sample color are not uniform over the sample surface, which does not allow application of conventional colorimetry for precise control of pharmaceutical tablets.

Recently, a technique for fast acquisition of the two-dimensional (2D) spatial distribution of reflectance spectra in a wide spectral range was proposed in our group [8]. It is based on the illumination of the object by a computer-controlled light source which generates fast-switchable predefined sequences of narrow spectral bands whose energy distribution is proportional to mutually orthogonal spectral functions. The acquisition of the 2D-distribution of reflectance spectra involves the assumption that these spectra can be approximated by a linear combination of just a few spectral functions [9,10]. These functions can be calculated by using the method of principle component analysis (PCA). In this work we utilized spectral functions calculated for the reflectance spectra of color chips from the Munsell book [11]. It was shown that more than 99% of 1257 reflectance spectra of these chips and various natural materials can be represented by using a linear combination of 6 – 8 bipolar spectral functions [12–14]. In this paper we describe a modified technique for 2D reflection-data acquisition, which is optimized for quantitative measurements of riboflavin concentration in tablets. The smooth reflectance spectrum of riboflavin [15] allows us to assume that the linear combination of 7 spectral functions is also sufficient for representation of its reflection spectrum. After measuring the response of our set of tablets with different riboflavin concentrations on the illumination with 7 spectral functions, we found one optimal spectral function which is enough for estimating the riboflavin content. It is shown that illumination of tablets by this optimal function allows us evaluate both the mean concentration of riboflavin and distribution of the concentration over the tablet (or tablets) surface.

2. Method and its optimization

2.1. Basic method

To obtain 2D- distribution of reflection spectra we illuminate a tablet (or a set of tablets) by a light source with a computer controlled radiation spectrum, and capture the object image by a black-and-white CMOS-camera. The light source consists of light-emitting diodes (LEDs) with different central wavelengths. By controlling the exposure time of every LED within the window needed for capturing one frame by the CMOS-camera, we can produce any desired pre-calculated illuminating spectral function with this light source [8]. In our experiment we used 7 spectral functions $S_k(\lambda)$, $k = 1 \dots 7$ calculated for optimal reconstruction of the spectral reflections of 1257 Munsell chips within the wavelengths range of 400 – 700 nm, which were published in [12]. These seven functions form an orthogonal basis. Six of them become negative within certain spectral regions as shown in Fig. 1. Illumination by these bipolar spectra was simulated by taking 2 measurements for each such spectral function: during the first frame the object was illuminated by light with spectrum from positive part of the spectral function, while during the second frame the light spectrum was switched to only negative part

of the same function [8]. Reconstruction of the image for complete bipolar spectral function was performed digitally by subtraction of second frame from the first one. The total number of captured images for each tablet was 13 because first orthogonal spectral function has only positive values, and other 6 were bipolar. Thus, seven 2D-distributions of the weighting coefficients $\sigma_k(x, y)$ have been obtained, one for each spectral function from the chosen orthogonal basis:

$$\sigma_k(x, y) = \int_{\lambda_1}^{\lambda_2} r(x, y, \lambda) S_k(\lambda) d\lambda \quad (1)$$

Here $r(x, y, \lambda)$ is reflectance spectrum of the object at surface coordinates of x and y , λ_1 and λ_2 are the boundary wavelengths of the spectral band (400 – 700 nm in our case). This set of σ_k -coefficients-images unambiguously represents approximate 2D-distribution of the reflectance spectra over the tablet surface [8]. On the one hand the measured distribution can be used for reconstruction of the reflection-spectra distribution using linear combination of the spectral functions $S_k(\lambda)$ weighted with the σ_k -coefficients. On the other hand, we can directly process the σ_k weighting coefficients for revealing the information how these spectra vary with changes of dye concentration in tablets.

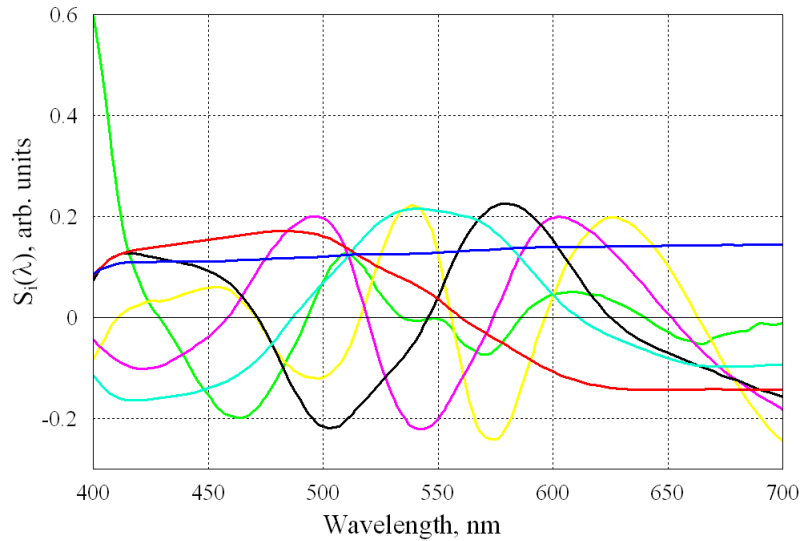


Fig. 1. Seven spectral functions $S_k(\lambda)$ computed from the measured Munsell color spectral data in Ref [12].

Assuming that change of the riboflavin concentration results in alteration of average reflectance spectra, we start comparison of different tablets by averaging the σ_k -coefficients over the central part of tablets, which covers about 90 per cent of their total area:

$$\bar{\sigma}_k = \frac{1}{A_S} \int_{A_S} \sigma_k(x, y) dS, \quad (2)$$

where A_S is the selected area of the tablet surface. These averaged coefficients $\bar{\sigma}_k$ form a vector in a 7 dimensional space. To avoid dependence on the average reflection of the object, on the distance between light source, object and camera, and also on the shape and position of the averaging area, a normalized 7D-vectors have been calculated:

$$v_k = \frac{\bar{\sigma}_k}{\sqrt{\sum_{k=1}^7 \bar{\sigma}_k^2}}. \quad (3)$$

These 7D-vectors represent averaged reflection spectra of different tablets in the compressed form, and they can be used for estimation of the dye concentration in tablets. In our particular case, the range of dye-concentration change was relatively small which allows us to assume the linear dependence of v_k -coefficients on the dye concentration η :

$$v_k = A_k \eta + B_k. \quad (4)$$

Note that coefficients A_k and B_k are different for different components of 7D-vector in both the magnitude and sign. They can be easily found by linear fit from the experimental data. When the coefficients A_k and B_k are defined, Eq. (4) can be used for estimation of the riboflavin concentration:

$$\eta = \frac{\sum_{k=1}^7 A_k (v_k - B_k)}{\sum_{k=1}^7 A_k^2} \quad (5)$$

Equation (5) shows that components of 7D-vector, which represent the reflectance spectrum of the object in the compressed form, are enough for calculation of dye concentration in tablet formulation. It is worth noting that the Eq. (5) can be used not only for calculation of the dye concentration in the averaged part of the tablet image but also for each pixel or a group of pixels. By this way the concentration distribution over the entire image of one or many tablets can be obtained.

Thus, multispectral imaging can be used to evaluate the dye concentration by taking a series images of tablets illuminated by computer controlled light source with pre-calculated spectral functions. However, the total number of captured images used for measurements is rather high (13) because two illuminations of tablets should be implemented for the most of spectral functions. In the next section we describe an optimized technique of the object illumination by a single spectral function, which diminishes the number of required captured images to just two.

2.2. Optimized method

The Eq. (5) can be transformed into simplified form:

$$\eta = C_0 + C_1 \sum_{k=1}^7 A_k v_k, \quad (6)$$

where C_0 and C_1 are constants:

$$C_0 = -\frac{\sum_{k=1}^7 A_k B_k}{\sum_{k=1}^7 A_k^2}; \quad C_1 = \frac{1}{\sum_{k=1}^7 A_k^2}. \quad (7)$$

Since $v_k = c_{norm} \bar{\sigma}_k$, where c_{norm} is the normalization constant in Eq. (3), one can rewrite Eq. (6) as following:

$$\eta = C_0 + c_{norm} C_1 \int_{\lambda_1}^{\lambda_2} R(\lambda) D(\lambda). \quad (8)$$

Here $R(\lambda) = \overline{r(x, y, \lambda)}$ is the reflection spectrum averaged over the chosen area of the object, and $D(\lambda)$ is new spectral function defined as

$$D(\lambda) = \sum_{k=1}^7 A_k S_k(\lambda). \quad (9)$$

This spectral function can be used for optimized detection of riboflavin. Using this function, only 2 measurements should be performed (for positive and negative parts of $D(\lambda)$) instead of 13 measurements when 7 orthogonal functions were used as it was described in the previous section. Indeed, defining two positive spectral functions for object illumination

$$D^+(\lambda) = \begin{cases} D(\lambda) & \text{if } D(\lambda) \geq 0 \\ 0 & \text{if } D(\lambda) < 0 \end{cases} \text{ and } D^-(\lambda) = \begin{cases} 0 & \text{if } D(\lambda) \geq 0 \\ -D(\lambda) & \text{if } D(\lambda) < 0 \end{cases}, \quad (10)$$

and using them for two-step measurements, two responses of CMOS camera averaged over the chosen area of the image can be obtained:

$$\sigma_{opt}^+ = \int_{\lambda_1}^{\lambda_2} R(\lambda) D^+(\lambda) d\lambda \text{ and } \sigma_{opt}^- = \int_{\lambda_1}^{\lambda_2} R(\lambda) D^-(\lambda) d\lambda. \quad (11)$$

Thereafter, it is useful to calculate the normalized value v_{opt} which is insensitive to variations of either illuminating conditions or distances between the light source, object, and camera:

$$v_{opt} = \frac{\sigma_{opt}^+ - \sigma_{opt}^-}{\sigma_{opt}^+ + \sigma_{opt}^-}. \quad (12)$$

As expected, this normalized response also possesses the linear dependence on the dye concentration in the tablet:

$$v_{opt} = a\eta + b. \quad (13)$$

Coefficients a and b in this case can also be found from the linear fit of the experimental data obtained for tablets with different and known-in-advance riboflavin concentration. Thus measuring of v_{opt} is sufficient for estimation of riboflavin concentration in any tablet. By calculating the normalized response of CMOS camera for smaller number of pixels of the captured image one can also obtain the distribution of the dye concentration over the entire image. Note that the image may contain either one tablet or several different tablets. In our experimental part we compare two methods of measuring v_{opt} . The first includes calculations of v_{opt} from the 13 images sequentially captured after object illumination by the set of orthogonal spectral functions using Eqs. (9-12). The second includes direct measurements of v_{opt} when the object is illuminated by two spectral functions of $D^+(\lambda)$ and $D^-(\lambda)$.

3. Materials and system descriptions

3.1. System description

Two dimensional multispectral images of the tablets were obtained using the system which is schematically shown in Fig. 2. The system includes a computer controlled light source and a CMOS camera which integrates all received luminous flux within frame duration. The light source consists of an array of conventional light emitting diodes (LEDs). We use 16 LEDs generating light at different wavelengths and covering the whole visible range from 400 nm to 700 nm. Each LED was coupled with a respective thin fiber (with a core of 910 μm). All thin

fibers are coupled with a single thick fiber (with a core of 5000 μm). Thick fiber is long enough (> 1 m) to provide efficient mixture of light at different wavelengths. The light emerged from the thick fiber is used for illumination of the object surface. The moments of switching on/off is controlled by the computer separately for each LED by means of specially designed electronic controller. As the illuminating time of each LED is controlled by a computer, an in-advance calculated spectral distribution of the light energy [such as proportional to any spectral function of $S_k(\lambda)$] can be readily generated.

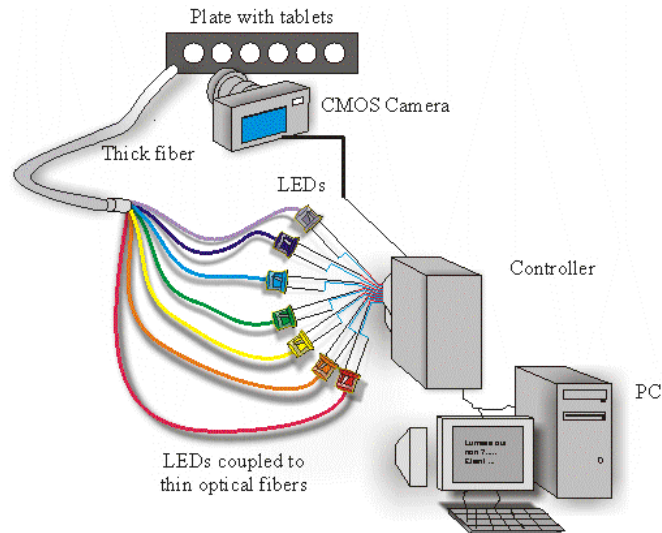


Fig. 2. Principle scheme of the system for fast acquisition of 2D distribution of the reflectance spectra.

In contrast with the system presented in [8,16], our new light source provides simultaneous illumination of the object by all necessary narrow spectral bands while precisely controlling the exposure time of each spectral band. The parallel mode of illumination reduces the response time of the system due to only one switching for a group of light emitting diodes (LEDs) instead of switching the LEDs sequentially. In this system the LEDs with relatively wide spectral bandwidth are used that leads to higher output optical power and decreases the measuring time in expense of the accuracy of implementation of the spectral function. Nevertheless, theoretical estimations show that increase of the lines bandwidth up to 20-30 nm maintains the ability of the system to distinguish small enough changes in the reflection spectra [17]. The light powers provided by different narrow spectral bands at the output of the thick fiber and their spectral bandwidth are shown in Fig. 3(b). As seen, both the maximal power and the bandwidth are varying from one LED to another. To implement the object illumination by an in-advance provided spectral function, we calculate duration of each LED switching so that the total exposure of the object provided by LEDs during one frame of the CMOS camera is proportional to either positive or negative part of the chosen spectral function. An example of the implementation of the third spectral function is illustrated in Fig. 3(a). The generation of any positive/negative parts of the illuminating spectral function is triggered by the synchronizing pulse from the CMOS camera in such a way that each camera frame is grabbed while the object is illuminated by different parts of the spectral functions. The light reflected from the tablets is collected into the monochrome CMOS camera by means of conventional C-mount lens. In our experiments, the camera rate of 2 frames per second was chosen to achieve the highest signal to noise ratio. It is defined by the combination of the light-source output power, illuminating area, and exposure time of the camera. All the frames are recorded in the personal computer for further processing. The luminous flux integrated by the CMOS camera during each frame is proportional to the object response on the illumination by the respective parts of the spectral function. After subtraction of two images

corresponding to the negative and positive parts, we obtain 2D distribution of the weighting coefficients $\sigma_k(x, y)$.

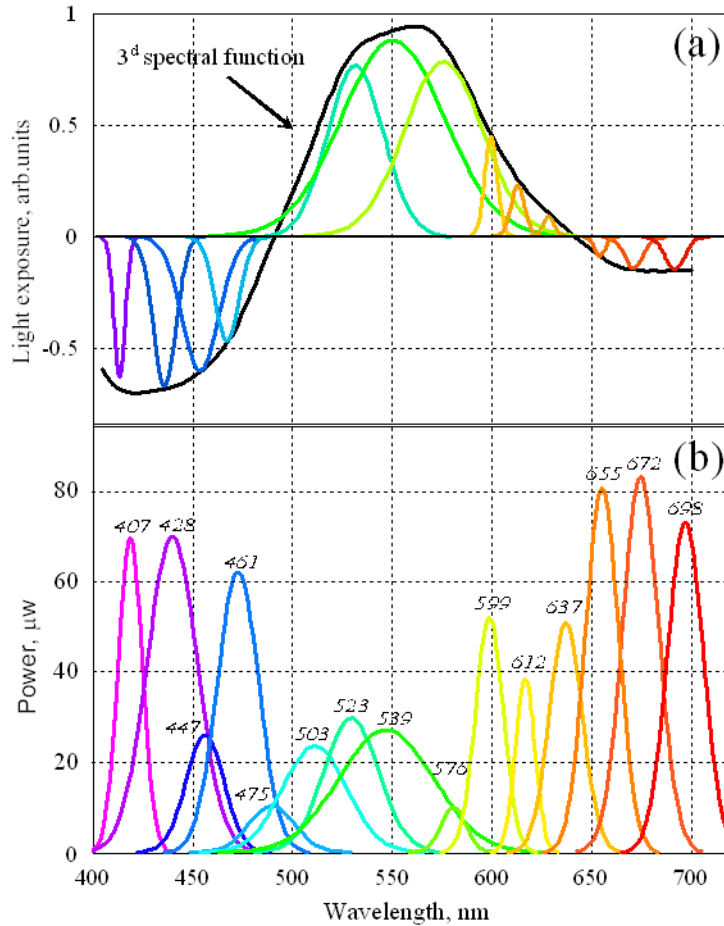


Fig. 3. (a) One of the spectral functions (third of seven) calculated in Ref [12], for the reflectance spectra of color chips from the Munsell book. (b) Output power of the LEDs from the thick fiber and their bandwidths as a function of the wavelength.

3.2 Materials

Tablets for the measurements were compacted with a compaction simulator (PUUMAN PCS-1) from six different mixtures of lactose monohydrate (Pharmatose 90M, DMV-Fonterra Excipients) and riboflavin sodium phosphate (Fluka Analytical). Desired mass basis riboflavin concentrations of the mixtures were from 3.5% to 6% with steps of a half percent. Each mixture was mixed in mortar in geometric series. The homogeneity of mixtures was measured by taking three samples from each mixture and analyzing the real concentration. The real concentrations of mixtures are described in Table 1.

Table 1. Riboflavin concentrations of the powder blends

Desired, %	Measured (mean), %	Error, %.
3.5	3.57	0.06
4	3.87	0.02
4.5	4.44	0.10
5	4.95	0.05
5.5	5.79	0.16
6	6.06	0.18

The compaction was carried out with a cylindrical die and 13-mm-diameter punches. A triangle wave compaction profile was used for upper punch, while lower punch was kept stationary. The compaction speed was 100 mm/s. Punches were prelubricated before every compaction with a 5% magnesium stearate (Orion Pharma) acetone solution. Before compaction 500 mg of lactose/riboflavin mixture was weighed for each tablet. Two tablets with minimal and maximal concentrations of riboflavin are shown in Fig. 4.

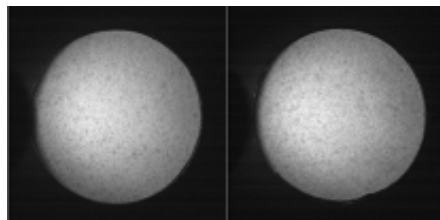


Fig. 4. Images of two tablets with maximal and minimal concentrations of riboflavin (3.5% in the left image and 6% in the right image) recorded under the day-light illumination.

Figure 4 shows that difference between two tablets under the day-light illumination is hardly distinguishable even for tablets with the largest difference of dye concentration.

4. Experiment and results

To demonstrate the feasibility of the proposed approach for measurements of the dye concentration in pharmaceutical tablets we used the setup schematically shown in Fig. 2. Each tablet was illuminated under the angle of incidence of 45 degree. The reflected light was collected into the CMOS camera under the normal incidence to the tablet. The technique of tablets illumination by the in-advance calculated spectral functions is described in the section 3.1. The difference of two adjacent frames recorded under illumination of the tablet by positive and negative part of the k -spectral function was calculated in the computer thus representing the distribution of $\sigma_k(x, y)$ weighting coefficients. By averaging the data of this distribution over the central area of the tablet image, which covers about 90 per cent of its total area, we get the value of $\bar{\sigma}_k$. After illumination by the complete set of orthogonal spectral functions we obtain all the components of the 7D-vector which characterizes the reflectance spectrum of the chosen part of the tablet in the compressed form. The measurements were repeated for the entire set of tablets with different riboflavin concentration shown in the Table 1. After the normalization of the measured data (see Eq. (3)), we found that each component ν_k is linearly dependent on the riboflavin concentration in the mixture these tablets were compacted from. Consequently, all the coefficients A_k and B_k in Eq. (4) were found. The riboflavin concentration was estimated using Eq. (5). The results of the concentration estimations are shown in Fig. 5 as a function of the concentration measured during the preparation of the tablets as described in Sect. 3.2. It is seen that small changes of

the averaged reflection spectra caused by 0.5% change of the riboflavin concentration are reliably detected by our system.

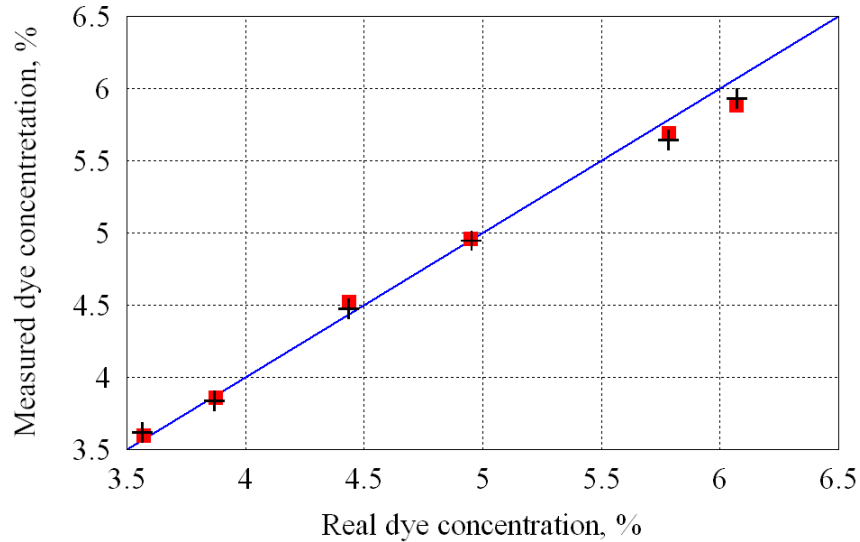


Fig. 5. Measured concentration of riboflavin in tablets as a function of their real concentration. Pluses are riboflavin concentrations measured optically by using tablets illumination with 7 orthogonal spectral functions, filled squares are concentrations measured by illuminating with the optimized spectral function of $D(\lambda)$.

In the next step we calculated the optimized spectral function $D(\lambda)$ (according to Eq. (9)) using experimentally found coefficients A_k for this set of tablets with different concentration of riboflavin. This spectral function is shown in Fig. 6. As one can see it has both the positive and negative parts. Illumination of the tablets by this spectral function was also implemented for measurements of the riboflavin concentration in the same set of samples. In this case only two CMOS-camera frames were used to carry out the measurements of each tablet instead of 13 when using 7 orthogonal spectral functions. First we illuminate the tablet by the positive part of function $D(\lambda)$ and then by its negative part. After subtraction of the image captured under illumination by $D^+(\lambda)$ from that captured under illumination by $D^-(\lambda)$ and normalization according to Eq. (12), we obtain the coefficient of v_{opt} . Here the camera responses were averaged over the same 90%-area of the tablet image as in the previous experiment. The measurements were repeated for all the tablets from the set. By this way we measured the coefficients v_{opt} for each tablet. These data also confirm the linear dependence of the measured v_{opt} on the real riboflavin concentration. It allows us to find the parameters a and b in Eq. (13) and use them later to estimate riboflavin concentrations which are plotted in the graph of Fig. 5 (filled squares).

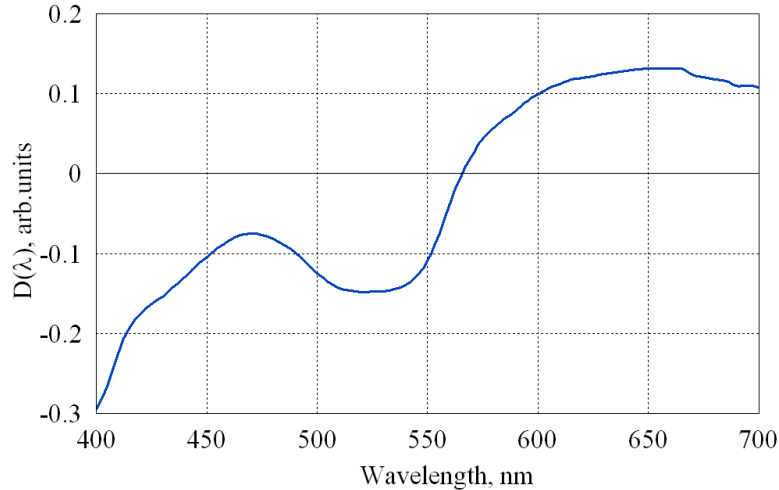


Fig. 6. The spectral function $D(\lambda)$ used for optimized illumination of tablets to measure the riboflavin concentration.

Differential pictures obtained after subtraction of the frames captured under illumination by the positive and negative parts of $D(\lambda)$ are shown in Fig. 7(a) for the boundary concentrations of riboflavin (3.5% and 6%). As one can see, the tablets with different concentration of riboflavin can be distinguished even by naked eye under the optimal illumination in contrast to images of Fig. 4 taken under conventional day-light illumination. For comparison we show in Fig. 7(b) images of the same tablets simulated in the computer from 13 frames captured when the tablets were illuminated by the set of mutually orthogonal spectral functions and calculated using Eqs. (6-12). As expected, both techniques show similar results. However, the technique of the illumination by the optimized spectral function is more preferable in practice because it may be implemented in a faster and simpler way.

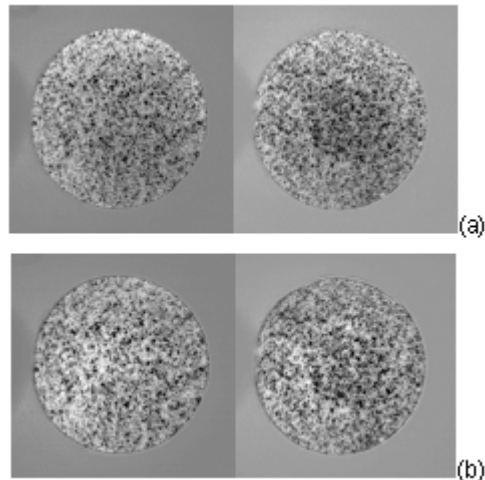


Fig. 7. Spatial distribution of riboflavin in two tablets with minimum and maximum concentrations of 3.5% (left) and 6% (right). The riboflavin is marked by black points, while the lactose – by white points. (a) – direct measurement of the tablet by their illumination with the optimized spectral function, (b) – computer simulation of the two-step optimal illumination by using 13 frames recorded under illumination by the set of 7 orthogonal spectral functions.

5. Conclusion

A method recently proposed for fast acquisition of the 2D spatial distribution of reflectance spectra in a wide spectral range has been applied for measurements of dye concentration in pharmaceutical tablets. The technique is characterized by fast measurements of small differences of reflectance spectra, which are caused by variations of dye concentration. It was found that the normalized parameter obtained after processing of the captured images linearly depends on the riboflavin concentration in the mixture these tablets were compacted from. After measuring the response of the available set of tablets with different riboflavin concentrations on the illumination with 7 mutually orthogonal spectral functions, we found an optimal spectral function which is enough for estimating the riboflavin content. The proposed technique of tablets illumination by the optimal spectral function allows us to evaluate both the mean concentration of riboflavin and distribution of the concentration over the tablet (or tablets) surface. This method can be applied for inspection systems and used under industrial environment in which real-time monitoring of dye concentration in each particular tablet is required.

Acknowledgements

The authors want to acknowledge the support of Promis Centre consortium, Promet project funded by the National Agency for Technology and Innovation (Tekes, decision number 70034/08) and collaborating companies. The financial support of the foundation for University of Eastern Finland formation is gratefully acknowledged. Partial financing of the Academy of Finland under the project No. 128582 is acknowledged. Authors also thank Consejo Nacional de Ciencia y Tecnología de México for financial support of sabbatical stay of Dr. Miridonov at the University of Eastern Finland.